Chapter 7

INFLUENCE OF PULSATILE WAVEFORMS ON THRESHOLD PREDICTIONS

The contents of this chapter is included in an article entitled:
Smit, J. E., Hanekom, T., Hanekom, J. J., van Wieringen, A. and Wouters, J. (2008) Effects of pulseshape on threshold and comfortable level predictions from a human auditory nerve fibre model containing persistent sodium and slow potassium currents, *submitted for publication*

7.1 INTRODUCTION

Macherey *et al.* (2007) recently developed a dual-process integrator-resonator phenomenological model of the human auditory nerve. The model assumed a population of 10,000 nerve fibres divided into two classes with half the population integrator ANFs and the other half resonator ANFs. In general, nerve fibres can be divided into a number of types, not to be confused with the Type I and Type II ANFs discussed in Chapter 2. The Type I nerve fibres exhibit integrator behaviour and Type II nerve fibres resonator behaviour (Izhikevich, 2007). The HH model is a resonator (Type II) model (Izhikevich, 2007) and hence it cannot fully explain the non-monotonic trends in ANF behaviour (Macherey *et al.*, 2007). Macherey *et al.* (2007) suggested that the voltage-gated ion channel currents that may explain these non-monotonic trends

are either a hyperpolarisation-activated current (I_h) already observed in mammalian spiral ganglion cells (Chen, 1997), or a combination of a slow potassium current and persistent sodium current (see for example the motor nerve fibre model by McIntyre, Richardson and Grill, 2002).

The ANF model described in Chapter 5 contains both persistent sodium and slow potassium currents. In this chapter the possibility is investigated that the ANF model will be able to predict threshold changes observed for different pulsatile waveforms. The objectives of the chapter are *a*) to verify the model against results from previous experimental studies; *b*) to determine the model's suitability to predict temporal characteristics of the different waveforms; and *c*) to investigate whether the combination of persistent sodium and slow potassium currents are sufficient to explain the non-monotonic trends observed in ANF behaviour.

7.2 MODEL AND METHODS

7.2.1 Stimuli and stimulation conditions

Simulations in this chapter were performed for a degenerate ANF population only, except for waveform rate simulations where both non-degenerate and degenerate populations are considered. Monopolar stimulation was simulated on a basal turn electrode from the contour (medial) array. Stimuli were charge-balanced and both anodic-first and cathodic-first pulse-train stimuli were considered. Phase durations for the high-amplitude short-duration phases of different stimuli were 40 μs/phase, except where stated differently, while the low-amplitude long-durations phases were eight times longer. Owing to the computational intensiveness of the model, stimuli were presented for 12 ms. Pilot calculations for stimuli presented at 12, 25, 50 and 100 ms indicated a threshold difference of less than 5% between stimuli presentations of 12 and 100 ms.

Simulations were performed for different pulsatile waveforms shown in Figure 7.1. Results were compared with experimental and model results from Macherey *et al.* (2006; 2007) and Van Wieringen *et al.* (2005; 2006). The nomenclature of the waveforms is the same as that provided by Van Wieringen *et al.* (2005) and Macherey

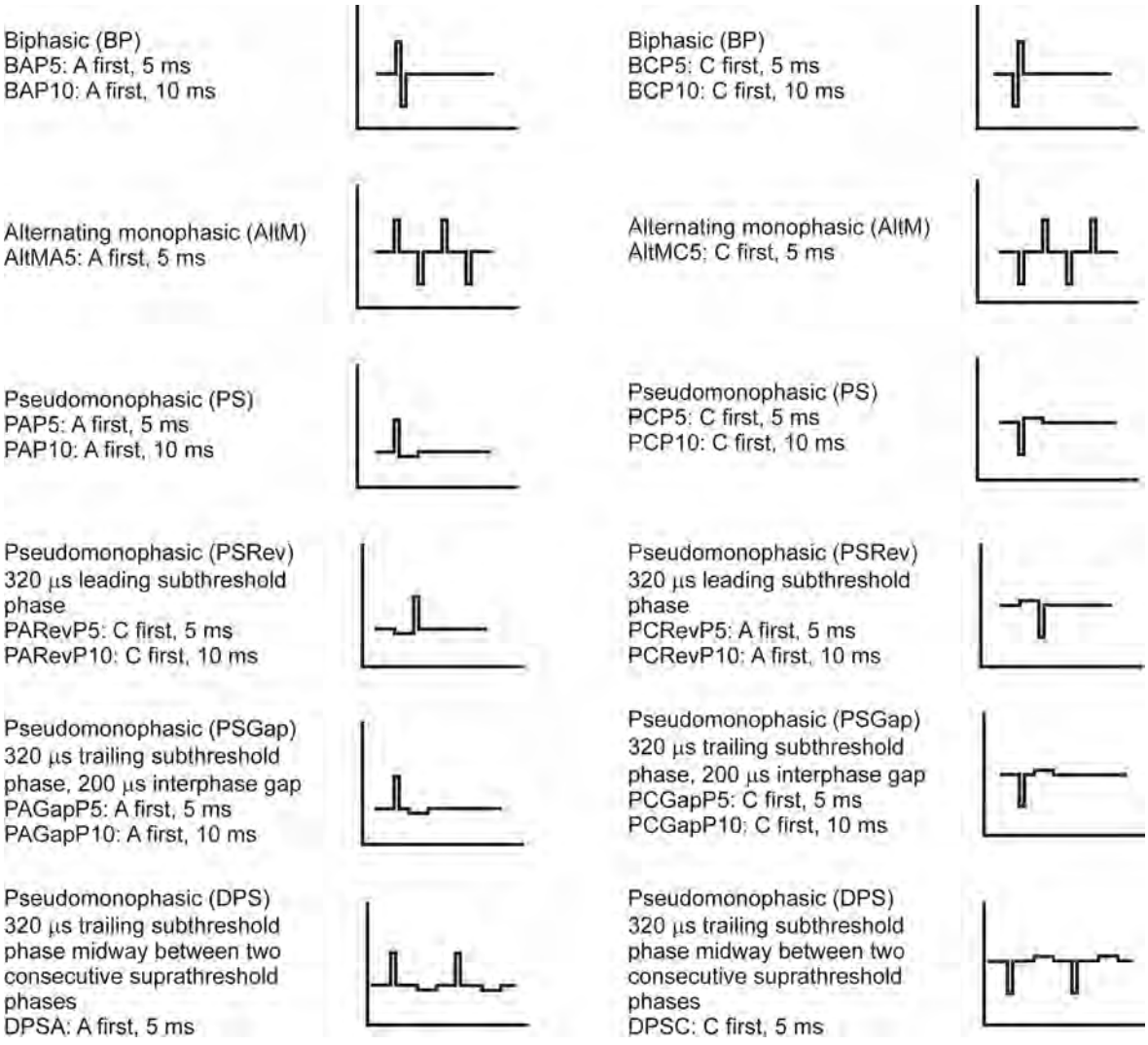

Figure 7.1: Overview of the different stimulus waveforms used to predict thresholds. The nomenclature is the same as that provided by Van Wieringen *et al.* (2005) and Macherey *et al.* (2006). Note that for the PSRev waveforms the polarity nomenclature in the name refers to the original PS waveform polarity, although the polarity is reversed.

et al. (2006). "BP" indicates a biphasic, "PS" a pseudomonophasic, "DPS" a delayed pseudomonophasic and "AltM" an alternating monophasic waveform respectively. Anodic-first stimulation is indicated by "A" and cathodic-first by "C". "P5" and "P10" refer to a 5.0 ms or 10.0 ms stimulation period respectively.

Phase durations for biphasic waveforms (BAP5, BCP5, BAP10 and BCP10) and alternating monophasic waveforms (AltMAP5 and AltMCP5) were 40 μs/phase. The high-amplitude short-duration phase of the pseudomonophasic waveforms (PAP5, PCP5, PAP10, PCP10) was 40 μs/phase, while the low-amplitude long-duration phase was eight times longer. The temporal effect of the two different phases of the pseudomonophasic waveforms was examined by reversing the two phases so that the low-amplitude long-duration phase leads (PARevP5, PCRevP5, PARevP10 and PCRevP10). Alternatively an interphase gap (IPG) of five times longer than the short-duration phase was introduced (PAGapP5, PCGapP5, PAGapP10, PCGapP10), as well as a longer IPG in the form of delayed pseudomonophasic waveforms (DPSAP5 and DPSCP5) as described by Macherey *et al.* (2006).

7.2.2 Threshold predictions

Thresholds were determined by calculating neural excitation curves for each stimulus waveform condition. The minimum threshold current for each curve was considered the threshold for the specific condition, with these minima located in close vicinity to the stimulating electrode.

Thresholds observed for different pulsatile waveforms differ widely among implantees as a result of variability in factors such as implant type, degree of degeneration of the ANF population, electrode geometry, intrascalar electrode location and stimulation strategy (Nadol Jr, 1990; Schuknecht, 1993; Zimmermann *et al.*, 1995; Nadol Jr, 1997; Arts *et al.*, 2003; Cohen *et al.*, 2003; Abbas *et al.*, 2004; Van Wieringen *et al.*, 2005; Fayad and Linthicum Jr, 2006). The model is hence only used to predict and compare relative threshold differences between different stimuli and not to predict thresholds differences observed in and between implantees.

7.3 RESULTS

7.3.1 Effect of electrode array position

Thresholds calculated for stimulation with the contour and straight electrode arrays respectively, using biphasic stimuli of 100 μs/phase, are shown in Figure 7.2. Threshold differences between different stimulus conditions and nerve fibre degeneracy were more pronounced with contour array stimulation than with straight array stimulation. It was therefore decided to consider only contour array stimulation in order to observe threshold differences between different pulsatile waveforms better.

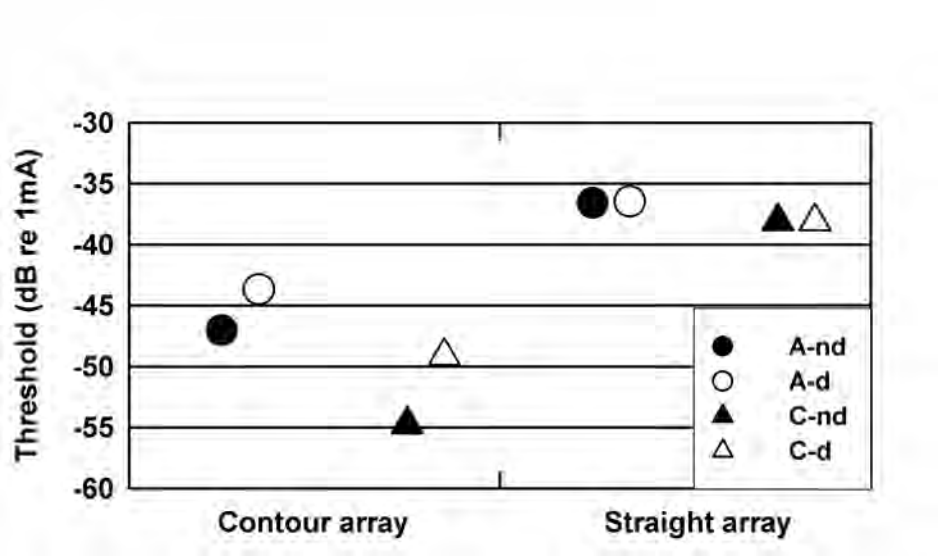

Figure 7.2: Thresholds determined for stimulation with the contour and straight electrode arrays respectively for non-degenerate (nd) and degenerate (d) ANF populations. Stimuli were charge-balanced and biphasic with 100 μs/phase phase durations and delivered to a monopolar stimulated electrode in the basal cochlear turn. Both anodic-first (A) and cathodic-first (C) stimuli were considered. Filled markers indicate non-degenerate and open markers degenerate nerve fibre populations. Anodic-first stimulation is indicated with circles and cathodic-first stimulation with triangles.

In general, cathodic-first stimuli produced lower thresholds compared to anodic-first stimuli in both non-degenerate and degenerate nerve fibre populations. With contour array stimulation, thresholds were 6.0 – 7.0 dB lower for cathodic-first stimuli. An increase in nerve fibre degeneracy elevated thresholds by 3.5 dB for cathodic-first

stimuli compared to 5.7 dB for anodic-first stimuli. With straight array stimulation, thresholds were about 1.5 – 2.0 dB lower for cathodic-first stimuli and nerve fibre degeneracy did not seem to influence threshold levels.

7.3.2 Effects of a low-amplitude long-duration phase

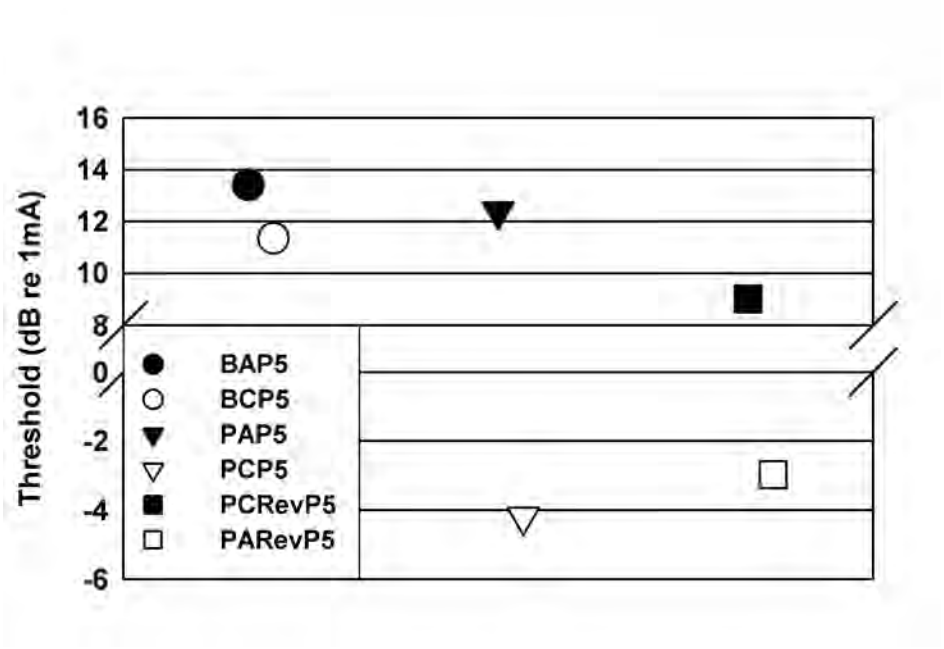

Figure 7.3: Threshold predictions for anodic-first (A) and cathodic-first (C) stimuli of biphasic waveforms (BAP5, BCP5) and pseudomonophasic waveforms with trailing (PAP5, PCP5) and leading (PARevP5, PCRevP5) subthreshold phases. Phase durations for high-amplitude short-duration phases were 40 μs/phase and 320 μs/phase for the low-amplitude long-duration phases. Pulse rates were 200 pps. Closed markers indicate anodic-first and open markers indicate cathodic-first stimuli.

The effectiveness of replacing either one of the phases of the BP waveforms with a pseudomonophasic phase of low amplitude and long duration was investigated. Figure 7.3 shows the threshold comparisons between biphasic (BAP5, BCP5), pseudomonophasic (PAP5, PCP5) and reversed pseudomonophasic (PARevP5, PCRevP5) waveforms for cathodic-first and anodic-first stimuli. Phase durations of the biphasic and high-amplitude short-duration phases of the PS and PSRev waveforms were 40 μs/phase, with the low-amplitude long-duration phases of the latter two waveforms 320 μs/phase.

For biphasic waveforms, thresholds for cathodic-first stimuli were 2.07 dB lower than for anodic-first stimuli. This is about 4.0 dB less than the same stimulus polarity threshold reductions predicted for the longer phase biphasic waveforms in Figure 7.2. The trend of a threshold reduction with increased phase duration compared favourably with similar measured results of threshold reductions ranging between 3.0 and 6.0 dB for PS waveforms reported previously for bipolar (Van Wieringen *et al.*, 2006) and a mean threshold reduction of 2.0 dB for anodic-first PS waveforms using monopolar stimulation (Macherey *et al.*, 2006).

Results further predicted a reduction in threshold for both stimulus polarities when one of the phases of the BP waveform was replaced with the prolonged phase. Replacement of the trailing phase resulted in thresholds being 1.02 dB lower for anodic-first and 15.54 dB lower for cathodic-first. Replacement of the leading phase of the BP waveform resulted in a threshold reduction of 14.33 dB for cathodic-first stimuli compared to only 4.41 dB for anodic-first stimuli.

In general, threshold reductions followed the same trends observed in the Van Wieringen *et al.* (2005) study. They observed lower thresholds for cathodic-first biphasic stimuli compared to anodic-first stimuli, as well as reduced thresholds for leading and trailing prolonged phase PS waveforms compared to BP waveforms. However, for three of the four subjects observed, anodic-first stimuli produce lower thresholds than cathodic-first stimuli in both types of PS waveforms. Threshold differences are also less pronounced than those predicted in this study.

7.3.3 Effects of an interphase gap

The effects of delaying the charge recovered from the leading phase were predicted through addition of a gap between the leading and trailing phases of BP and PS waveforms. For the BP waveforms of rate 200 pps (i.e. BP waveforms having a 5.0 ms stimulation period), a gap of 5.0 ms was inserted between the two phases. This resulted in alternating monophasic (AltM) waveforms of rate 100 pps (i.e. having a stimulation period of 10.0 ms). For PS waveforms two such alternations were made by *a*) inserting a 200 μs gap between the two phases; and *b*) delaying the low-amplitude long-duration trailing phase to be halfway between two consecutive high-amplitude short-duration leading phases.

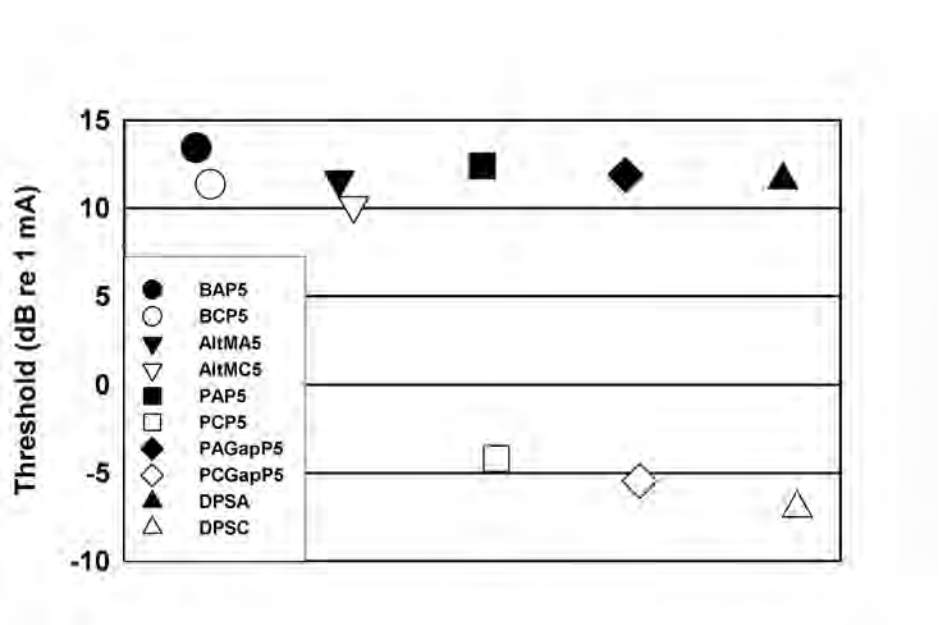

Figure 7.4: Threshold predictions for increasing the interphase gap of BP and PS waveforms. BP and PS stimuli are the same as presented in Figure 7.3. Predictions were made for anodic-first (A) and cathodic-first (C) stimuli of alternating monophasic (AltMA5, AltMC5), pseudomonophasic (PAGapP5, PCGapP5) with a 200 μs interphase gap and delayed pseudomonophasic (DPSA, DPSC) waveforms. Waveform parameters are the same as in Figure 7.3.

In the Van Wieringen *et al.* (2006) study threshold reductions range between 5.0 and 8.0 dB in the case of AltM waveforms for bipolar stimulation, while for monopolar stimulations a mean reduction of about 18.0 dB is observed for both anodic-first and cathodic-first stimuli (Macherey *et al.*, 2006). Predicted threshold reductions are shown in Figure 7.4. In the case of AltM waveforms of both stimulus polarities, only small threshold reductions were predicted and ranged between 1.21 and 1.82 dB. Increasing the IPG of PS waveforms also resulted in increased threshold reductions. Reductions were more pronounced for cathodic-first stimuli, being 1.27 dB lower for PSGap and 2.81 dB lower for DPS. For anodic-first stimuli reductions ranged between 0.51 and 0.79 dB. Compared to experimental results, these reductions were less than expected.

7.3.4 Effect of an increase in the interpulse interval

Interpulse intervals (IPIs) for BP and PS waveforms were increased from 5 ms to 10 ms, while all other waveform parameters were kept constant. The effect of the IPI increase on both anodic-first and cathodic-first stimuli is shown in Figure 7.5.

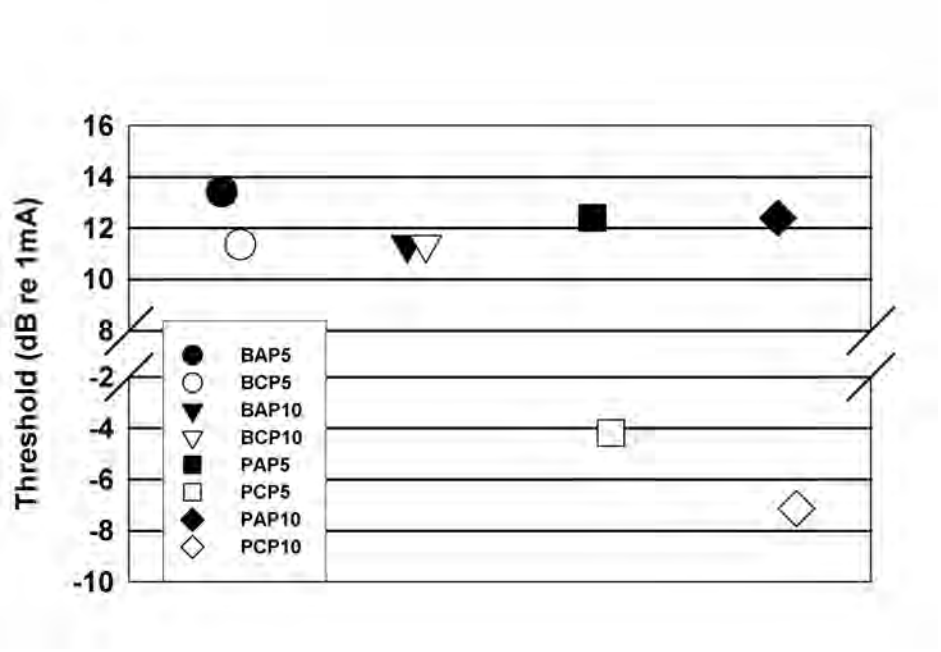

Figure 7.5: Threshold predictions for increasing the interpulse interval of anodic-first (A) and cathodic-first (C) BP and PS waveforms from 5 ms to 10 ms. BP and PS stimuli, as well as waveform parameters, are the same as in Figure 7.3.

For the BP waveform anodic-first stimulation resulted in a 2.07 dB reduction in threshold, while the reduction predicted for cathodic-first stimulation was negligible. These small threshold differences are comparable to the results of Van Wieringen *et al.* (2005) and Macherey *et al.* (2006), indicating threshold changes with an IPI increase of 5 ms of less than 1.0 dB for bipolar and less than 3.0 dB for monopolar anodic-first stimulation.

Increasing the IPI of the PS waveform resulted in a threshold reduction of 2.94 dB for cathodic-first and a negligible reduction for anodic-first stimulation, indicating an opposite threshold dependence on stimulus polarity compared to BP waveforms. Macherey *et al.* (2006) observed no significant threshold dependence on polarity for

PS and DPS waveforms, with threshold differences between the two polarities less than 1.0 dB.

7.3.5 Comparison between measured and modelled results

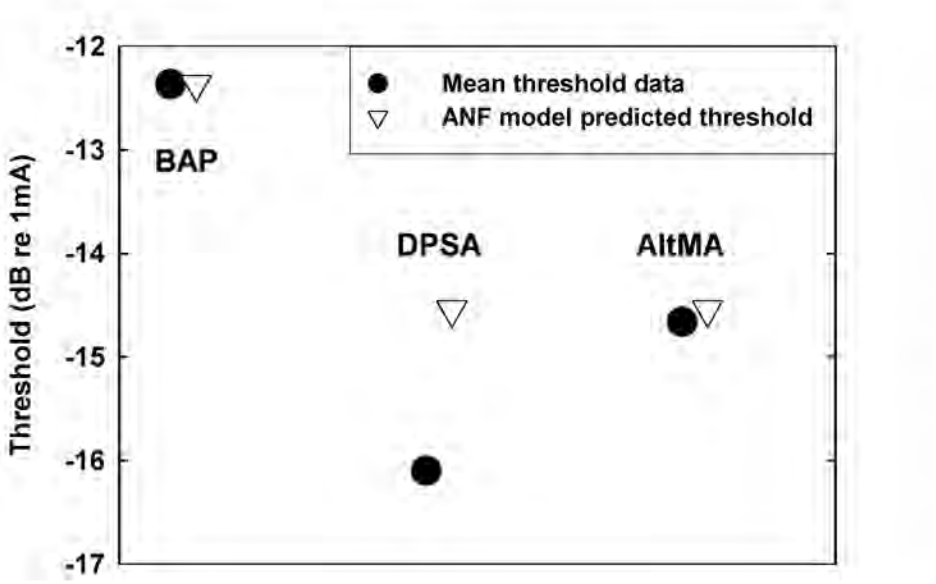

Figure 7.6: Threshold comparisons between predicted ANF model and observed mean threshold data reproduced from Figure 10 in Macherey *et al.* (2006) for anodic-first stimuli of BP, DPS and AltM. For the Macherey *et al.* (2006) data (closed markers) the high-amplitude short-duration phase is 21.6 μs, the low-amplitude long-duration phase is 172.4 μs, and the rate is 813 pps for the BP and DPS waveforms and 407 pps for the AltM waveform. For the ANF model predictions (open markers) the high-amplitude short-duration phase is 40.0 μs, the low-amplitude long-duration phase is 320.0 μs, and the rate is 800 pps for the BP, 200 pps for the DPSA and 400 pps for the AltM waveforms.

All of the above results were model predictions of tendencies observed when varying the parameters of biphasic and asymmetric waveform shapes. Of interest is how well the model can predict measured results. All simulations in this study were performed for a monopolar electrode configuration and the model predictions cannot be arbitrarily referenced to the biphasic anodic-first reference waveforms of the Van Wieringen *et al.* (2005) study that employed a bipolar electrode configuration. However, Macherey *et*

al. (2006) employed monopolar stimulation and ANF model predictions could hence be arbitrarily referenced to their biphasic anodic-first reference stimuli.

Comparisons between anodic-first BP, DPS and AltM waveforms are illustrated in Figure 7.6. Phase duration and stimulus rate values are indicated in the figure legend, with phase durations of the Macherey *et al.* (2006) stimuli about half of the modelled stimuli. Given the threshold differences predicted when varying phase duration, IPG and IPI, the model was able to make reasonable predictions of general trends measured for mean thresholds from human subjects. Pulse rates for the DPSA stimuli used in the Macherey *et al.* (2006) study were four times faster than pulse rates employed in the simulations. The difference between the measured and calculated thresholds for the DPSA waveforms may be attributed to refractory period differences between real and simulated ANFs, as discussed below in Section 7.4.

7.3.6 Effects of pulse rate

Pulse rate effects on thresholds were studied by Van Wieringen *et al.* (2006) and Macherey *et al.* (2007) for BP and AltM waveforms at different phase durations. Results show a monotonic decrease in threshold for the BP waveform over the pulse rate range investigated, while non-monotonic behaviour is observed at low pulse rate AltM waveforms. Shannon (1985) also observed non-monotonic trends in threshold behaviour for BP waveforms over a wider range of pulse rates than those in the Van Wieringen *et al.* (2006) study.

Pulse rate effects were investigated with the ANF model over the range 200 – 5,000 pps for BP and AltM waveforms of 40 μs/phase durations for non-degenerate and degenerate nerve fibres (Figures 7.7(a) and (b)). Results were arbitrarily referenced to a 200 pps BP reference waveform. This was performed by determining a guestimate of the threshold that a measured 200 pps BP waveform of 40 μs/phase would have from Figures 3b and 5 in Van Wieringen *et al.* (2006). Fayad and Linthicum Jr (2006) reported a mean spiral ganglion cell count in 14 implanted temporal bones of about 67% less than that known to be in normal hearing persons (Schuknecht, 1993). Mean threshold curves for the two waveforms were thus calculated from Figures 7.7(a) and (b) by assuming a mixed population of 33% non-degenerate and 67% degenerate nerve fibres (Figures 7.7(c) and (d)).

In general thresholds were higher for degenerate compared to non-degenerate nerve fibres (Figures 7.7(a) and (b)). Results indicated threshold reductions for both BP and AltM waveforms at pulse rates higher than 1,000 pps, although the average reduction of 1.3 dB/doubling predicted for the mean BP waveform was less than the 3.6 dB/doubling predicted for the AltM waveform (Figures 7.7(c) and (d)). For BP waveforms having pulse rates less than 1,000 pps, thresholds did not follow the trend of a monotonic decrease with increasing pulse rate. Results also did not predict the non-monotonicities observed at low pulse rate AltM waveforms.

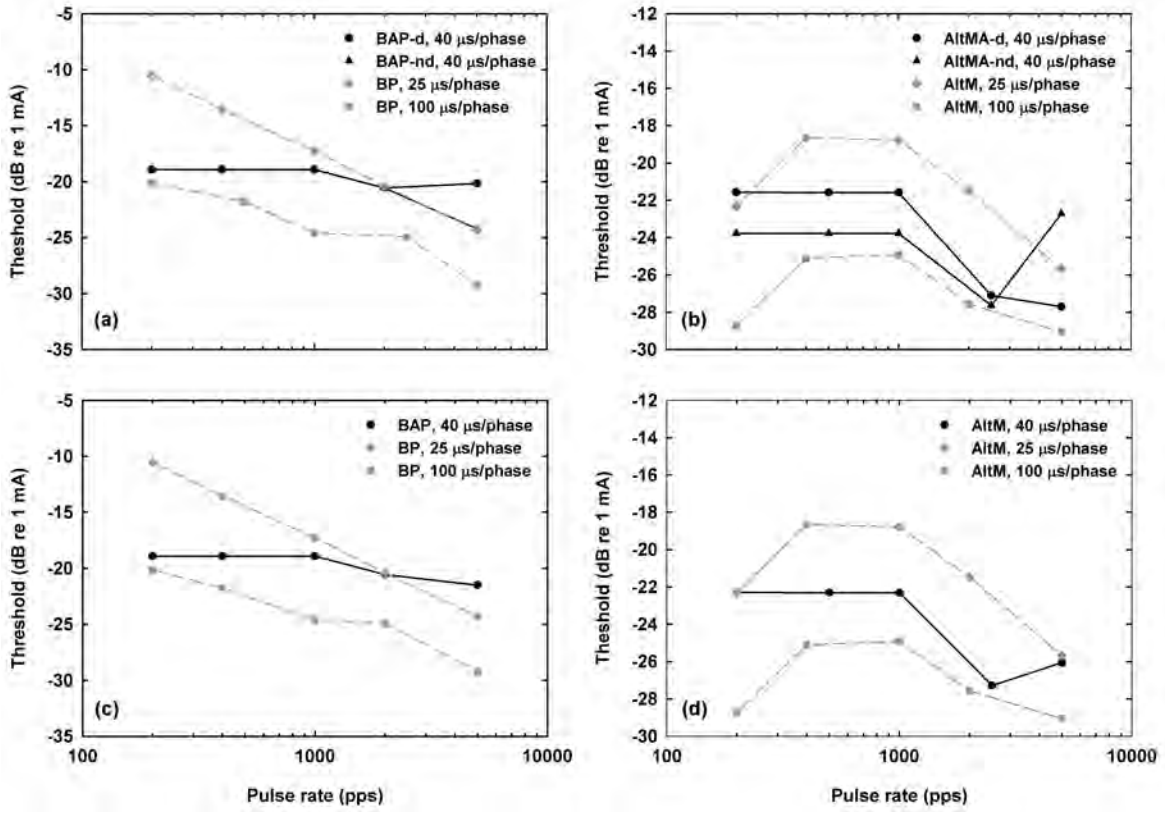

Figure 7.7: Thresholds as a function of pulse rate of (a, c) BP and (b, d) AltM waveforms at 25, 40 and 100 μs/phase durations for anodic-first stimuli. The experimental results at 25 and 100 μs/phase are reproduced from Figure 5 in Van Wieringen *et al.* (2006) and are indicated in grey (dashed lines). (a, b) Thresholds at 40 μs/phase were calculated for non-degenerate (*nd*, black solid lines, triangles) and degenerate (*d*, black solid lines, circles) nerve fibres. (c, d) Mean thresholds were calculated from (a) and (b) by assuming a mixed nerve fibre population of 33% non-degenerate and 67% degenerate nerve fibres.

7.4 DISCUSSION

In this chapter the possibility is investigated that the ANF model is able to predict threshold changes observed for different waveform shapes of different polarity, phase duration and pulse rate. Stimulation was monopolar for a contour array electrode located in the basal turn of the modelled cochlea.

Deurloo, Holsheimer and Bergveld (2001) investigated the threshold-distance relationship between a monopolar electrode and mammalian nerve fibres with a 3D volume conduction model by analysing the effect that presentation of subthreshold prepulses, i.e. pulses similar to the PS waveform, have on the nerve fibre's electrical behaviour. They stated that "the two basic relations of the stimulus current needed for nerve fibre activation are: (1) the current is inversely related to the calibre of the myelinated nerve fibre and (2) the current increases approximately proportional to the square of the distance between the nerve fibre and the stimulating electrode .... These two relations imply that with a given stimulus amplitude, larger fibres will be activated up to a larger distance from the cathode than smaller fibres. Therefore, larger fibres will be activated in a larger area of a nerve trunk than smaller fibres."

The first relation is in part based on a report by McNeal (1976) that, because of their longer internodal lengths, nerve fibres having a larger calibre, i.e. a larger diameter, are excited at lower threshold currents than thinner fibres. Simulation studies by Wesselink *et al.* (1999) and Rattay (1990) are in accord with this observation. As discussed in Chapter 5, the axonal part of the ANF model is based on the general peripheral sensory nerve fibre model developed in Chapters 3 and 4. In Sections 4.3.6 and 4.4 evidence was provided that the general sensory nerve fibre model is not in full accord with the abovementioned results, since for larger diameter fibres (larger than 10.0 μm) an increase in threshold current occurred with an increase in diameter. However, in the smaller diameter regime in which ANF fibre diameters fall, the general nerve fibre model, and hence the ANF model as well, complied with the first relation.

Single-fibre studies by Ranck Jr (1975) and model results by, among others, Rattay (1990) indicate that the threshold current increases with the square of the distance from the electrode, complying with the second relationship stated above. The electric and potential fields become weaker as the electrode-to-fibre distance increases, with the result that larger threshold stimulus currents are necessary to excite the fibre at larger

distances. This has the effect that as the fibre distance from the electrode increases, the excitation region around the electrode increases, since more Ranvier nodes fall inside the depolarised region. In cochlear implant research both experimental and modelling studies reported lower thresholds for fibres located closer to the stimulating electrodes, with the greatest reduction for fibres lying closest to the electrodes (Javel *et al.*, 1987; Miller *et al.*, 1993; Shepherd *et al.*, 1993; Hanekom, 2001b; Briaire and Frijns, 2006). These results are also supported by the results presented in Figure 7.2, with thresholds for fibres obtained with contour array stimulation reduced compared to straight array stimulation.

From the two relationships presented by Deurloo *et al.* (2001) it can be argued that when a stimulating monopolar electrode is located an equal distance from the dendrite on the one hand and the axon on the other, the axon would be excited at lower threshold currents than the dendrite. Current-distance relationships calculated for a myelinated nerve fibre confirm this argument (refer to Figure 6 in Rattay, 1987). However, the difference predicted in Figure 7.2 between non-degenerate and degenerate ANFs cannot be explained by this argument alone. The situation in the cochlea is more complicated owing to the spatial arrangement of fibres (refer for example to the cross-sectional diagram of the modelled cochlea employed in this study, as shown in Figure 5.2). From Figure 5.2 it is clear that each ANF is shaped in a curved fashion, with the dendrites in general located closer to the electrode array than the axons, even more so for ANFs located close to an electrode compared to ANFs located between two consecutive electrodes. Since retrograde degeneration causes the dendrites to retract, while the somas and axons survive (Spoendlin and Schrott, 1989; Nadol Jr, 1990; Schuknecht, 1993), excitation in degenerate fibres is expected to occur more centrally along the fibre, i.e. axonal excitation. It can therefore be deduced that thresholds predicted for non-degenerate fibres located close to the stimulating electrode will be lower than for degenerate fibres. This is clearly observed in the case of contour array stimulation, but not in the case of straight array stimulation. The reason is found in the way the ANF is modelled. The dendritic part of the Rattay *et al.* (2001b) model, which is assumed myelinated, is reserved in the ANF model (refer to Figure 5.1). This is in contrast to real ANFs where the dendrites are mostly unmyelinated (Glueckert *et al.*, 2005a). Furthermore, comparison between the internodal lengths of the dendrite and axon shows longer dendritic than axonal internodal lengths. In myelinated fibres located closely to electrodes, the threshold current is mainly dependent on the electrode-to-node distances and not so much on the electrode-to-fibre distance as is

the case of unmyelinated fibres (refer to Figure 6 in Rattay, 1987). Threshold currents are also lower when the electrode is located at a node compared to when it is located between nodes. The straight array is located closer to the terminal of the ANF than the contour array (refer to Figure 5.2) and therefore has to excite a larger part of the dendrite in a non-degenerate fibre to create a propagating AP. The degenerate fibre was simulated with almost no dendrite left (Figure 5.1) and excitation occurred in the axon. Since the nodes of the axon are spaced close together, lower thresholds currents might be expected than for dendritic excitation, but the additional electrode-to-fibre distance increases the threshold current. This is confirmed by the results shown in Figure 6 in Rattay (1987), where simulations predicted similar thresholds at longer electrode-to-fibre distances for a myelinated fibre of double the diameter to thresholds predicted in the thinner fibres when the electrode is located closer to the node in the former case than in the latter.

Thresholds are reported to be dependent on electrode configuration with monopolar stimulation in cats and guinea-pigs yielding lower thresholds than bipolar stimulation (Black and Clark, 1980; Black *et al.*, 1983; Miller *et al.*, 1995; Rebscher *et al.*, 2001). Lower thresholds are also recorded for monophasic stimuli compared to BP stimuli in single-fibre and ECAP studies performed by Miller *et al.* (1995; 1999b; 2001b) on cats and guinea-pigs. Miller *et al.* (2003) measured the growth in ECAP amplitudes in cats employing monophasic and BP stimuli for both monopolar and bipolar stimulation modes. Results indicate larger threshold differences between the monophasic and BP stimuli for monopolar stimulation than for bipolar stimulation. They attributed the threshold differences to the difference in voltage gradient produced by the two stimulation modes. With a monopolar electrode a single potential gradient is produced, while bipolar stimulation produces two gradients. Simulations performed with 3D spiralling cochlear models also indicate two potential gradients of opposite sign (Briaire and Frijns, 2000; Hanekom, 2005). Miller *et al.* (2003) hence argued that with a bipolar electrode pair nerve fibres close to one of the electrodes will always be excited, irrespective of the type of stimulus presented. They reasoned that for monopolar stimulation a BP waveform will introduce a second polarity, and hence the change in the potential field will be greater than for a monophasic waveform, leading to the larger observed threshold differences. Increasing the duration of the second phase of BP stimuli, i.e. stimulation with PS stimuli, leads to a relatively large reduction in threshold compared to BP stimuli (Miller *et al.*, 1995; Shepherd and Javel, 1999; Miller *et al.*, 2001b; Van Wieringen *et al.*, 2005; Macherey *et al.*, 2006). Furthermore, reversal

of stimulus polarity resulted in larger observed threshold differences when monophasic stimulation was used (Miller *et al.*, 1999b), compared to the differences observed with BP stimuli (Shepherd and Javel, 1999).

Predicted threshold reductions shown in Figure 7.3 for BP waveform replacement with PS waveforms followed the trend of larger threshold reductions for monopolar stimulation than for bipolar stimulation. Lower thresholds were also predicted for PS waveforms compared to BP waveform for both stimulus polarities. However, the threshold differences between BP and AltM waveforms shown in Figure 7.4 were less than experimentally observed for both bipolar and monopolar stimulation (compare with Van Wieringen *et al.*, 2005; Macherey *et al.*, 2006). This may be attributed to the refractory periods of the modelled ANF. Calculated ARP values of about 0.8 – 0.9 ms were 44% longer than the measured ARP values of 0.5 ms for humans, while the calculated RRP values were 15 – 23% shorter than RRP values of about 5.0 ms (compare Section 5.3.2 and Brown *et al.*, 1990). The results in Figure 7.3 were for low pulse rate predictions and from the effect pulse rate has on thresholds, presented in Figure 7.7, it can be deduced that the longer ARP value of the modelled ANF resulted in an overestimation of thresholds for low pulse rate AltM waveforms. This can be explained as follows: For each anodic-cathodic phase-pair in the AltM stimulus, the leading anodic phases hyperpolarise the membrane, thus lowering the fibre's threshold. The lower threshold enables the trailing cathodic phases to depolarise the membrane more easily to elicit an AP. However, with low pulse rate pulses, the membrane has time to recover from the hyperpolarised state before it is depolarised. If the AP is elicited during the ARP time window, the AP amplitude will be too low to propagate. Hence, the threshold current needed to elicit a propagating AP will be raised.

Thresholds recorded for monopolar simulation display dependence on stimulus polarity with single-fibre studies by Van den Honert and Stypulkowski (1987b) and ECAP studies by Miller *et al.* (1998; 1999b; 2001a) recording lower thresholds for cathodic stimuli than for anodic stimuli in cats. However, in guinea-pigs the situation is reversed, with anodic stimuli yielding lower thresholds (Miller *et al.*, 1998). The threshold differences in the cat studies may be attributed to the observation that cathodic stimuli excite fibres more distally than anodic stimuli do, although the influence the soma plays is unclear (Miller *et al.*, 1999b). No preference is observed between the stimulus polarities with bipolar stimulation (Miller *et al.*, 2003). Calculated thresholds in this study were in accord with observations on stimulus polarity for monopolar stimulation in

cat. However, simulations were performed for a degenerate ANF population and stimulus polarity differences could hence not be attributed to the difference in stimulation site between the two polarities. As discussed earlier in this section, the combination of contour array stimulation and ANF degeneracy most probably resulted in axonal stimulation irrespective of stimulus polarity. The calculated differences might rather be the result of the way in which the two polarities depolarises the fibre (Rattay, 1987). However, this was not investigated further and additional study in this regard is advised.

Subthreshold prepulses similar to PSRev waveforms, but with both phases having a cathodic polarity, have been investigated as a possible way to stimulate nerve fibres in a nerve trunk selectively (Grill and Mortimer, 1995; Grill and Mortimer, 1997; Deurloo *et al.*, 2001). Simulation reports indicate an inversion of the threshold-distance relationship with lower thresholds observed for fibres located further away from the electrode, and those within a certain distance from the electrode threshold currents for small nerve fibres are lower than for thicker nerve fibres. The authors argued that a possible mechanism for these simulation predictions is two-fold. Firstly, the prepulse activates a certain percentage of the sodium channels at the Ranvier nodes closest to the electrode, thus reducing the sodium conductance. When the actual pulse stimulates the nerve fibre, the resulting AP has a reduced amplitude. Secondly, the threshold current needed to activate the nodes is elevated to such an extent that the neighbouring nodes are strongly hyperpolarised and hence the AP is blocked from propagating. Comparison between the neural excitation curves for PCP5 and PARevP5 waveforms showed a shift in the position of the minimum threshold predicted for the PARevP5 waveform away from the stimulating electrode compared to the PCP5 waveform (results not shown). However, an investigation into the sodium conductance reduction mechanism links up with the stimulus polarity investigation suggested in the previous paragraph as a further study.

Shannon (1985) measured thresholds in humans for BP waveforms of varying pulse rate and phase duration using monopolar stimulation. Thresholds are reduced with an increase in phase duration. Furthermore, for short phase durations (< 0.5 ms), thresholds are constant for pulse rates up to 100 pps, after which it decreases by about 3 dB/octave (see Figure 1 in Shannon, 1985). Van Wieringen *et al.* (2006) observed similar non-monotonical behaviour with an increase in pulse rate for BP and AltM stimuli. For BP stimuli reported thresholds reduce between 1.6 and 2.6 dB/doubling

of rate for pulse rates between 200 and 5,000 pps. Threshold reductions for AltM stimuli vary between 1.1 and 2.0 dB/doubling of rate over the same range of pulse rates. Shannon (1985) suggested that two different mechanisms are at play for short and long pulse durations respectively, with the long pulse duration mechanism being an integrator process with a 1 – 2 ms time constant. He referred to results from Pfingst and Sutton (1983) reporting that low frequency thresholds, i.e. long pulse duration thresholds, in monkeys correlate with dendritic survival near the stimulating electrode. Thresholds are elevated in regions of degenerate nerve fibres, and hence poor dendritic survival, compared to regions with more intact nerve fibres with more dendritic survival. Furthermore, he referred to the suggestions made by Van den Honert and Stypulkowski (1984) of two sites of activation on the nerve fibre relative to the soma and that dendrites integrate current slower than the soma with a time constant of 1 – 2 ms. Shannon (1985) argued that these findings suggest that the higher thresholds observed for lower frequency, i.e. long pulse duration, stimuli can be attributed to low dendritic survival.

Macherey *et al.* (2007) expanded the Carlyon *et al.* (2005) phenomenological model and reported that simulated predictions of the stochastic model version are able to follow the trends observed in the Shannon (1985) study, but not for the deterministic version. Van den Honert and Stypulkowski (1984), among others, observed a reduction in jitter, and hence in stochastic behaviour, when the amount of degeneracy of nerve fibres is increased, while Miller *et al.* (1999b) recorded greater jitter for longer pulse durations in cats and a reduction in jitter with an increase in FE. This suggests that for long pulse durations less jitter, and hence dendritic activity, will result in higher observed thresholds. Thus it can be argued that the stochastic Macherey *et al.* (2007) model does not simulate a population of non-degenerate nerve fibres only, but rather a mixed population of degenerate and non-degenerate nerve fibres. The inability of the deterministic version of the Macherey *et al.* (2007) model to predict the Shannon (1985) results of threshold reductions with an increase in pulse rate, may be an indication of either an underestimation of thresholds at low pulse rates or an overestimation of thresholds observed at higher pulse rates. In the former case, the lower threshold predictions at lower pulse rates will then suggest that their deterministic model possibly simulates mostly a population of non-degenerate nerve fibres.

The dual-process model by Macherey *et al.* (2007) consists of integrator and resonator

processes. They showed that the non-monotonicities can be attributed to the resonant process. They argued that even though the HH model is a resonator model, the model's ion channels are insufficient to account for the non-monotonicities experimentally observed, since the model's time constants are too small. The ion channels responsible for the correct time constants may be a combination of persistent sodium and slow potassium currents. The ANF model used in this study was a deterministic model containing persistent sodium and slow potassium currents. It could be used to simulate non-degenerate and degenerate nerve fibres. Figure 7.7 shows that the model was able, within reason, to predict the non-monotonic behaviour in thresholds for pulse rates higher than 1,000 pps, confirming the suggestion by Macherey *et al.* (2007).

However, at low pulse rate BP waveforms the ANF model underestimated thresholds and at high pulse rates overestimated thresholds. The model also did not correctly predict the threshold changes observed for low pulse rate AltM waveforms. This can be attributed partly to a difference in the refractory periods between real and simulated ANFs as discussed previously. In addition, the inclusion of stochastic behaviour in the model would enable modelling of the relationship between jitter and FE mentioned earlier. Hence, it could possibly better predict the threshold differences observed at low pulse rates between non-degenerate and degenerate nerve fibres. The development of a stochastic version is therefore advised.

7.5 CONCLUSION

In conclusion it seems possible that the human ANF model is able to make a reasonable prediction of temporal characteristics of different biphasic, pseudomonophasic and alternating monophasic waveforms, as well as the non-monotonic behaviour observed at high pulse rates. Since the model contained both persistent sodium and slow potassium currents, it is suggested that the inclusion of these currents can in part simulate non-monotonic behaviour in ANFs. However, these non-monotonic trends observed cannot be explained by the combination of persistent sodium and slow potassium currents alone. Results indicate that other possible contributing factors include refractory behaviour of the nerve fibre and the stochastic representation of the ion channels at the Ranvier nodes.